

## CRYSTALLIZATION PAPERS

*Acta Cryst.* (1998). D54, 86–89

### Crystallization and structure solution of p53 (residues 326–356) by molecular replacement using an NMR model as template

PEER R. E. MITTL,\* PATRICK CHÈNE and MARKUS G. GRÜTTER at Core Drug Discovery Technologies, Ciba-Geigy AG, CH-4002 Basel, Switzerland. E-mail: mittl@fmi.ch

(Received 9 January 1997; accepted 29 April 1997)

#### Abstract

The molecular replacement method is a powerful technique for crystal structure solution but the use of NMR structures as templates often causes problems. In this work the NMR structure of the p53 tetramerization domain has been used to solve the crystal structure by molecular replacement. Since the rotation- and translation-functions were not sufficiently clear, additional information about the symmetry of the crystal and the protein complex was used to identify correct solutions. The three-dimensional structure of residues 326–356 was subsequently refined to a final *R* factor of 19.1% at 1.5 Å resolution.

#### 1. Introduction

The tumor suppressor p53 protein needs to form tetramers for tight binding to DNA. Deletions or mutations of the p53 tetramerization of p53 is an important factor that effects correct of the protein to DNA (Waterman *et al.*, 1995). The tetramerization of p53 is an important factor that effects proper binding to the recognition site. It was shown that *in vitro* monomeric p53 does not bind to DNA, while dimeric and tetrameric p53 do (Shaulian *et al.*, 1993; Tarunina & Jenkins, 1993; Waterman *et al.*, 1995; Zhang *et al.*, 1994). The functional role of p53 tetramerization is supported by the observation that in human cancers, where p53 is very often mutated, the tetramerization domain is not effected (reviewed by Soussi & May, 1996). The NMR structure of the p53 tetramerization domain was analyzed independently by two groups (Clore *et al.*, 1994, 1995; Lee *et al.*, 1994). The crystal structures of residues 325–356 and residues 319–360 were determined at 1.7 Å (Jeffrey *et al.*, 1995) and 2.5 Å resolution (Miller *et al.*, 1996), respectively.

Molecular replacement is a powerful and rapid technique for the solution of crystal structures provided preliminary structural information is available. Small protein structures are often determined by NMR prior to X-ray crystallography since the NMR method avoids the often difficult step of protein crystallization. The NMR structure could subsequently be used for preliminary phasing by molecular replacement. Unfortunately this approach often fails for several reasons. Conformational and thermal differences between X-ray and NMR structures exert decreased signal-to-noise ratios in the rotation and translation functions. Particularly for small proteins or peptides, where NMR has advantages over X-ray crystallography, the problems are aggravated by the fact that these crystals are often densely packed and the structures have a non-globular elongated shape. Here we describe how the crystal structure of a 31-mer peptide from the p53 oligomerization domain (residues 326–356) was solved by molecular replace-

ment using the NMR model of Lee *et al.* (1994) as a search template.

#### 2. Materials and methods

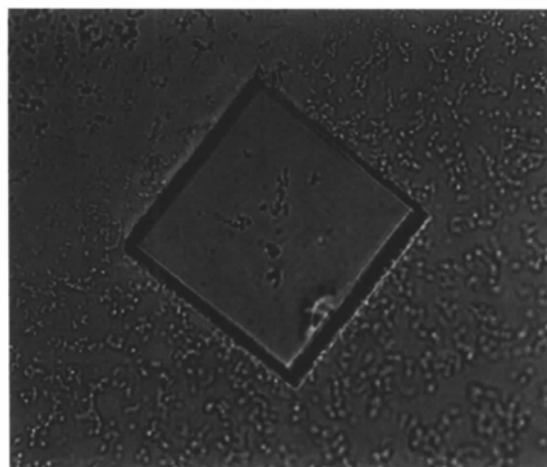
##### 2.1. Crystallization and data collection

Recombinant p53 was produced and purified as described elsewhere (Chène, Mittl & Grütter, 1998). Three different crystal forms of the p53 tetramerization domain were grown using the hanging-drop method under very similar conditions. The reservoir solution consisted of 1.4 *M* sodium citrate and 100 mM HEPES, pH 7.9–8.1. In most of the crystallization experiments at least two crystal forms were observed in the same drop. The crystal forms could be distinguished by their different crystal habits (Fig. 1). The presence of 0.5%  $\beta$ -octylglucoside improved the size of the crystals and favored the formation of one crystal species over the other. Table 1 gives an overview regarding the different crystal forms. Since the tetragonal crystals diffracted X-rays to the highest resolution we collected data from this crystal form at the ESRF in Grenoble (France) at the Swiss–Norwegian beamline. The wavelength of the X-rays was set to  $\lambda = 0.875$  Å and the MAR image-plate detector was positioned at a distance of 183 mm. Each data-frame covered 1° and was exposed for 3 min. Data were processed with *XDS* (Kabsch, 1988). The analysis of the data set indicated a steeper decrease of the average intensity along the *c\** axis than in the *a\*/b\** plane. Statistics for the data are given in Table 1.

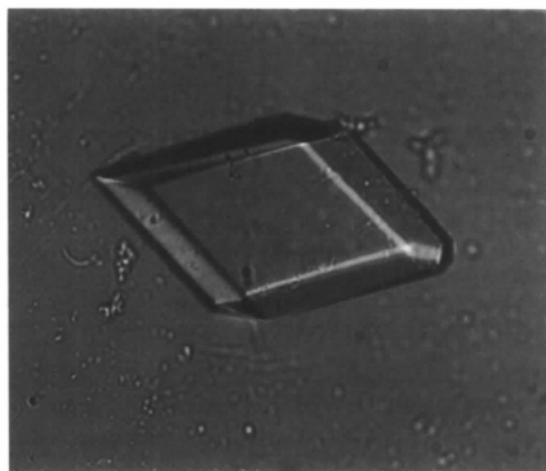
##### 2.2. Structure solution and refinement

This data set was subsequently used to solve the structure by molecular replacement. Since the X-ray structure of the p53 tetramerization domain was not available at that time (Jeffrey *et al.*, 1995), we had to use the NMR model of Lee *et al.* (1994) as a search model. All steps of the structure solution were calculated with the program *AMoRe* (Navaza, 1994). Initially we attempted to solve the structure by placing the properly rotated search model manually on one of the special positions with subsequent rigid-body refinement of the orientation. Because of the differences between the search model and the final crystal structure and the limited radius of convergence of the rigid-body refinement method this approach failed, and we proceeded in the following way.

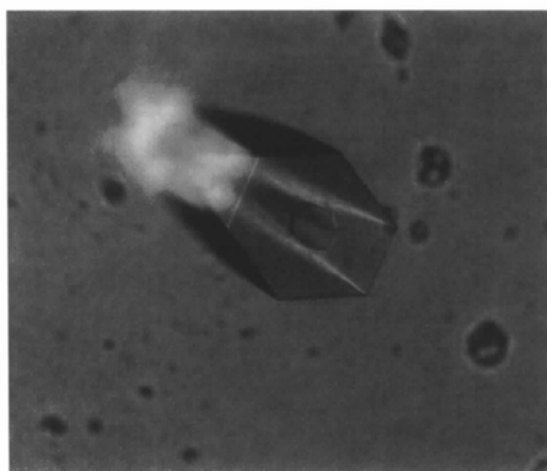
The 19 structures of the NMR model (Brookhaven accession code 1PET; Lee *et al.*, 1994) were superimposed onto the first structure using the program *O* (Jones *et al.*, 1991). In the next step a complete tetramer was created consisting of 76 copies of residues 325–355 and all side-chain atoms were deleted. The center of gravity of the search model was moved to the origin



(a)



(b)



(c)

Fig. 1. Crystals of the p53 tetramerization domain (residues 326–356). Three different crystal forms have been observed: (a) tetragonal, (b) trigonal and (c) hexagonal (see Table 1).

and the twofold axes were aligned parallel to the unit-cell axis of a  $P1$  cell (cubic cell,  $a = 70 \text{ \AA}$ ). The cross-rotation function was calculated for the resolution range 20–4.0  $\text{\AA}$  with a patterson radius of 12  $\text{\AA}$ . The 16 highest peaks from the rotation function varied between  $2.90\sigma$  and  $1.75\sigma$  and were used for the calculation of the translation function. Among this list there were many peaks with rotations around  $0^\circ$ ,  $90^\circ$ ,  $180^\circ$  or  $270^\circ$ . The translation function was calculated for the resolution range 10.0–4.0  $\text{\AA}$ . For each rotation the ten best solutions were listed.

Since we expected a monomer in the asymmetric unit, the tetrameric search model could only obtain certain rotations and translations. We therefore screened the list of 160 peaks for solutions that possessed the following criteria:  $\alpha, \beta, \gamma \in (0, 90, 180, 270^\circ) \pm 1^\circ$ ;  $\Delta a, \Delta b, \Delta c (0.0, 0.5) \pm 0.01$ ;  $R_f < 60\%$ . These solutions are given in Table 2 and were subjected to rigid-body refinement at a resolution range of 10.0–4.0  $\text{\AA}$ . Before rigid-body refinement all solutions had nearly identical correlation coefficients ( $r$ ) and  $R$  factors (around 20 and 58% respectively). After 15 cycles of rigid-body refinement the correlation coefficients and  $R$  factors of two solutions were significantly improved (solutions 1 and 2 in Table 2) compared with the other five solutions. Both solutions transformed the search model into different asymmetric units of the crystal and produced the same packing.

The resulting electron-density map was sufficiently clear to incorporate the p53 sequence starting with residues 326–356. The model was further refined by alternating rounds of molecular dynamics (program *X-PLOR*; Brünger *et al.*, 1987) and manual interventions (program *O*; Jones *et al.*, 1991). In order to account for the anisotropic diffraction the data was corrected according to the method of Sheriff & Hendrickson (1987). The  $R$  factor converged at 19.1% for all data between 8.0 and 1.5  $\text{\AA}$  resolution. During the refinement 40 water molecules and alternative side-chain conformations for residues 327, 329, 335 and 342 were included into the structure. The r.m.s.d.'s for bond lengths and angles were 0.010  $\text{\AA}$  and  $1.17^\circ$ , respectively. Fig. 2 shows the final  $\sigma_A$ -weighted  $2F_o - F_c$  electron density for residues 331–338. The coordinates and structure factors have been deposited with the Protein Data Bank.†

### 3. Results and discussion

Three different forms of crystals with markedly distinguishable habits have been observed. The tetragonal and hexagonal crystals have very similar unit-cell parameters to the crystals reported by Jeffrey *et al.* (1995). The trigonal crystal form has been reported by Miller *et al.* (1996). Since the tetragonal crystals diffracted much better than the others, they were selected for the structure determination.

NMR structures often give weak rotation-function solutions, therefore different strategies have been suggested to emphasize the correct solution. Both methods downweight parts with high structural flexibility and increase the signal from rigid parts. Kleywegt (1996) suggests calculating structure factors from a set of superimposed NMR structures with uniform  $B$  factors rather than the energy-minimized structure alone, while Wilmanns & Nilges (1996) determined pseudo  $B$  factors from

† Atomic coordinates and structure factors have been deposited with the Protein Data Bank, Brookhaven National Laboratory (Reference: 1AIE, 1AIESF). Free copies may be obtained through The Managing Editor, International Union of Crystallography, 5 Abbey Square, Chester CH1 2HU, England (Reference GR0714).

Table 1. Crystals of p53 tetramerization domain and statistics of data collection

Values in parentheses are those for the outermost shell (1.6–1.5 Å) whereas those not in parentheses are for the whole resolution range (26.9–1.5 Å).

Crystal form	Tetragonal	Trigonal	Hexagonal
Habit	Square-like plates	Trigonal prisms	Hexagonal rods
Size (mm)	0.3 × 0.3 × 0.05	0.2 × 0.2 × 0.4	0.2 × 0.2 × 0.5
Space group	<i>P</i> 422	<i>P</i> 3 <sub>1(2)</sub> 21	<i>P</i> 6 <sub>1(5)</sub> 22
Unit-cell dimensions (Å, °)	<i>a</i> = <i>b</i> = 45.5, <i>c</i> = 33.2, α = β = γ = 90	<i>a</i> = <i>b</i> = 50.1, <i>c</i> = 117.2, α = β = 90, γ = 120	<i>a</i> = <i>b</i> = 80.6, <i>c</i> = 50.4, α = β = 90, γ = 120
<i>d</i> <sub>max</sub> (Å)	1.5	3.5	6
Resolution (Å)	26.9–1.5 (1.6–1.5)		
Completeness (%)	94.6 (90.7)		
<i>R</i> <sub>sym</sub> (%)	6.9 (42.1)		
Percentage <i>I</i> ≥ 3σ (%)	76.0 (50.0)		
Unique reflections	5740 (852)		
Multiplicity	5.0 (4.8)		

Table 2. Molecular replacement solutions before and after rigid-body refinement

No.	Rotation and translation parameters before rigid-body refinement						Before rigid-body refinement		After rigid-body refinement	
	α	β	γ	Δ <i>a</i>	Δ <i>b</i>	Δ <i>c</i>	<i>r</i>	<i>R</i> <sub>f</sub>	<i>r</i>	<i>R</i> <sub>f</sub>
1	0.00	180.00	90.31	0.001	0.504	0.000	20.3	58.2	58.3	49.6
2	90.31	0.00	0.00	0.999	0.498	0.000	20.2	58.2	58.1	49.8
3	0.00	180.00	0.30	0.005	0.499	0.000	20.2	58.3	48.9	53.9
4	0.00	180.00	180.31	0.995	0.501	0.000	20.3	58.2	48.8	53.2
5	360.30	0.00	0.00	0.993	0.501	0.000	20.2	58.3	45.0	55.8
6	0.00	180.00	270.31	0.000	0.501	0.000	20.2	58.2	43.8	50.0
7	270.31	0.00	0.00	0.000	0.497	0.000	20.3	58.2	43.2	51.9

a set of NMR structures. In the case of large structures, the first method is often not applicable due to software limitations, but in the case of p53 it was the method of choice. Although the crystals contained only one monomer in the asymmetric unit we were not able to determine a useful signal from a monomeric search template under any set of conditions tested, most likely because of the elongated shape of the search model (dimensions

30 × 20 × 10 Å) that increased the noise level of the rotation function. A tetrameric search model had a more globular shape (dimensions 40 × 40 × 30 Å) that should give less noisy maps. Nevertheless, the correct rotation-function solutions yielded only 1.75σ peaks which were much weaker than the global maximum (2.90σ). Patterson correlation refinement (Brünger, 1990) was unable to emphasize the correct solutions.

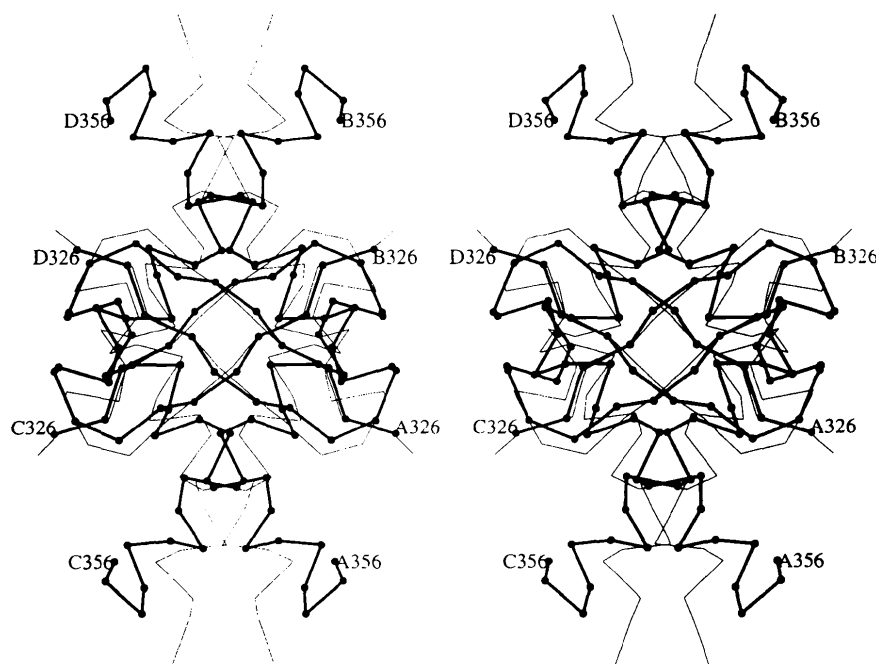


Fig. 2. Stereo plot of the final  $\sigma_A$ -weighted  $2F_o - F_c$  electron density for the turn between  $\beta$ -sheet and  $\alpha$ -helix (residues 331–338). The map was contoured at  $1.5\sigma$ . The side chain of Glu336 possesses the highest thermal mobility of the whole structure.

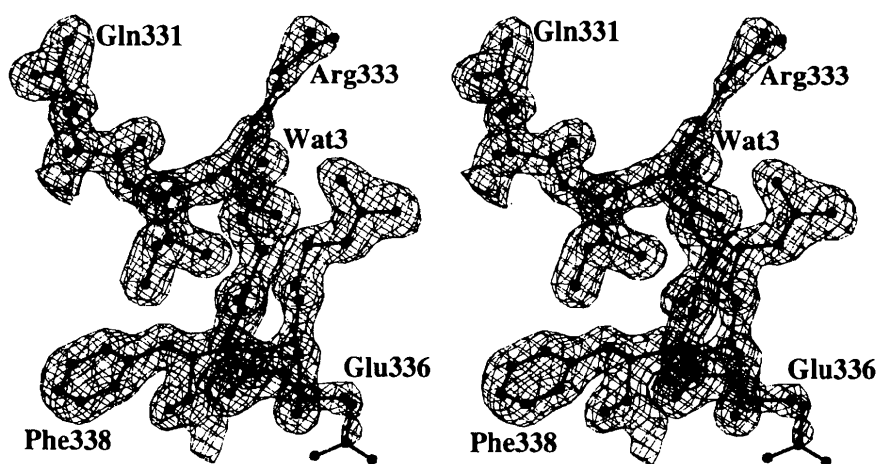


Fig. 3. Superposition of the tetrameric NMR search model (thin lines) onto the final crystal structure (bold lines with bullets). The four chains are labelled *A–D*. Although we used a set of 19 superimposed NMR structures as a search template, we have depicted the energy-minimized NMR structure to visualize the differences.

The correct rotation and translation function solutions could only be selected because of additional information on how the tetramer should be located in the crystal. In space group *P422* all twofold axes run parallel to unit-cell axes and three twofold axes intersect at either  $(\frac{1}{2}, 0, \frac{1}{2})$ ,  $(0, \frac{1}{2}, 0)$ ,  $(\frac{1}{2}, 0, 0)$  or  $(0, \frac{1}{2}, \frac{1}{2})$ . Since the tetrameric search model was centered at the origin and pre-aligned with its twofold axes parallel to the unit-cell axes, the correct rotation could only be a multiple of  $90^\circ$  and the correct translation must be close to one of the special positions. All solutions listed in Table 2 fulfill these requirements and possess very similar *R* factors and correlation coefficients before rigid-body refinement. Nevertheless only two of them could be refined to reveal correct solutions.

As described previously, the structure of the p53 tetramerization domain consists of one  $\beta$ -strand (residues 326–333) and one  $\alpha$ -helix (residues 335–356). Two symmetry-related  $\beta$ -strands form an antiparallel  $\beta$ -sheet (Lee *et al.*, 1994; Jeffrey *et al.*, 1995; Clore *et al.*, 1995; Chène *et al.*, submitted). Although we used all 19 NMR structures for molecular replacement, we superimposed only the energy-minimized NMR structure on the final X-ray structure, in order to simplify the presentation of the differences between the search template and the final model. The *C $\alpha$*  r.m.s.d. for the superposition of the entire tetramer is 2.3 Å (residues 326–355 from each chain) which is reduced to 1.4 Å if the superposition is made, based on a single monomer. It becomes evident from Fig. 3 that the  $\beta$ -sheets fit nicely onto each other, but the  $\alpha$ -helices possess different orientations relative to each other (Fig. 3). We conclude that we would not have been able to solve this structure by molecular replacement without the additional knowledge of the symmetry of the tetramer. Such information is of great value in molecular replacement and should always be considered if possible.

### References

- Brünger, A. T. (1990). *Acta Cryst.* **A46**, 195–204.  
 Brünger, A. T., Kuriyan, J. & Karplus, M. (1987). *Science*, **235**, 458–460.  
 Chène, P., Mittl, P. R. E. & Grütter, M. G. (1998). *J. Mol. Biol.* In the press.  
 Clore, G. M., Ernst, J., Clubb, R., Omichinski, J. G., Kennedy, W. M., Sakaguchi, K., Appella, E. & Gronenborn, A. M. (1995). *Nature Struct. Biol.* **2**, 321–333.  
 Clore, G. M., Omichinski, J. G., Sakaguchi, K., Zambrano, N., Sakamoto, H., Appella, E. & Gronenborn, A. (1994). *Science*, **265**, 386–391.  
 Jeffrey, P. D., Gorina, S. & Pavletich, N. P. (1995). *Science*, **267**, 1498–1502.  
 Jones, T. A., Zou, J.-Y., Cowan, S. W. & Kjeldgaard, M. (1991). *Acta Cryst.* **A47**, 110–119.  
 Kabsch, W. J. (1988). *J. Appl. Cryst.* **21**, 916–924.  
 Kleywegt, G. J. (1996). *Jnt CCP4/ESF-EACBM Newslett. Protein Crystallogr.* **32**, 32–36.  
 Lee, W., Harvey, T. S., Yin, Y., Yau, P., Lichfield, D. & Arrowsmith, C. H. (1994). *Nature Struct. Biol.* **1**, 877–890.  
 Miller, M., Lubkowski, J., Mohana Rao, J. K., Danishefsky, A. T., Omichinski, J. G., Sakaguchi, K., Sakamoto, H., Appella, E., Gronenborn, A. M. & Clore, G. M. (1996). *FEBS Lett.* **399**, 166–170.  
 Navaza, J. (1994). *Acta Cryst.* **A50**, 157–163.  
 Shaulian, E., Zauberman, A., Milner, J., Davies, E. A. & Oren, M. (1993). *EMBO J.* **12**, 2789–2797.  
 Sheriff, S. & Hendrickson, W. A. (1987). *Acta Cryst.* **A43**, 118–121.  
 Soussi, T. & May, P. (1996). *J. Mol. Biol.* **260**, 623–637.  
 Tarunina, M. & Jenkins, J. R. (1993). *Oncogene*, **8**, 3165–3173.  
 Waterman, J. L., Shenk, J. L. & Halazonetis, T. D. (1995). *EMBO J.* **14**, 512–519.  
 Wilmanns, M. & Nilges, M. (1996). *Acta Cryst.* **D52**, 973–982.  
 Zhang, W., Guo, X. Y. & Deisseroth, A. B. (1994). *Oncogene*, **9**, 2513–2521.